Spectral and Energy Efficiency of Line-of-Sight OAM-MIMO Communication Systems

Rui Chen, *Member, IEEE,* Hong Zhou, Wen-Xuan Long and Marco Moretti, *Member, IEEE*

***Abstract*—Not only high spectral efficiency (SE) but also high energy efficiency (EE) are required for future wireless communication systems. Radio orbital angular momentum (OAM) provides a new perspective of mode multiplexing to improve SE. However, there are few studies on the EE performance of OAM mode multiplexing. In this paper, we investigate the SE and EE of a misaligned uniform concentric circle array (UCCA)-based multi-carrier multi-mode OAM and multiple-input multiple-output (MCMM-OAM-MIMO) system in the line-of-sight (LoS) channel, in which two transceiver architectures implemented by radio frequency (RF) analog synthesis and baseband digital synthesis are considered. The distance and angle of arrival (AoA) estimation are utilized for channel estimation and signal detection, whose training overhead is much less than that of traditional MIMO systems. Simulation results validate that the UCCA-based MCMM-OAM-MIMO system is superior to conventional MIMO-OFDM system in the EE and SE performances.**

***Index Terms*—Orbital angular momentum (OAM), uniform concentric circle array (UCCA), spectral efficiency (SE), energy efficiency (EE).**

I. Introduction

Recently, orbital angular momentum (OAM) carried by vortex electromagnetic waves with helical phase fronts [1], [2] provides a new perspective for high data rate wireless transmission. Due to the inherent orthogonality between OAM modes, multiplexing a set of orthogonal OAM modes on the same frequency channel can achieve high capacity and spectral efficiency (SE) [3]. Moreover, combining OAM mode multiplexing with conventional multiple-input multiple-output (MIMO) technology can result in higher capacity gain [4]. On the other hand, energy efficiency (EE), defined as the ratio of the capacity to the total system power consumption, has been recognized as a important performance metric of green communication systems. There are a number of researches dedicated to the EE of MIMO systems [5], [6], but few for OAM systems. To the best of our knowledge, only the authors in [7] analyze the EE of the OAM spatial modulation (OAM-SM) communication system. Due to the high SE of OAM relying on mode multiplexing, it is therefore necessary to investigate the EE and SE performances of mode-multiplexed or multi-mode OAM communication systems.

The EE of a communication system is dependent on the structure of the transceiver and antennas. There are several methods that can be used to generate radio OAM waves [8], among which uniform circular array (UCA) is the most popular because of the ubiquity of antenna array in wireless communication systems and its ability to control wavefronts. The feasibility of utilizing UCA to generate single-mode and multi-mode OAM waves has been verified in [2], [9]. To generate single-mode OAM waves, all the antenna elements in a UCA are fed with the same input signal, but with a successive phase shift from element to element such that after a full turn the phase has the increment of $2\pi\ell$, where ℓ is an unbounded integer termed as topological charge or OAM mode number [1]. For multi-mode OAM waves, there are two transmitter architectures, implemented by RF analog synthesis and baseband digital synthesis respectively [10]. Since mode and space multiplexing gains could be simultaneously harvested to further improve the SE through combining OAM and MIMO with uniform concentric circular array (UCCA) [11], we focus on the corresponding RF analog and baseband digital transceiver architectures as shown in Fig. 1.

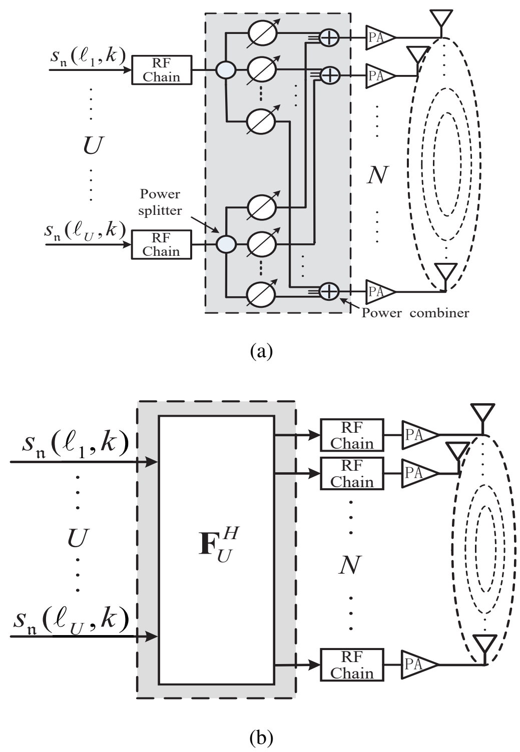

Fig. 1: The UCCA-based multi-mode OAM transmitter implemented by (a) RF analog synthesis, and (b) baseband digital synthesis.

Rui Chen, Hong Zhou and Wen-Xuan Long are with the State Key Laboratory of ISN, Xidian University, Shaanxi 710071, China (e-mail: rchen@xidian.edu.cn, hzhou_1@stu.xidian.edu.cn).

Marco Moretti is with the University of Pisa, Dipartimento di Ingegneria dell'Informazione, Italy (e-mail: marco.moretti@iet.unipi.it).

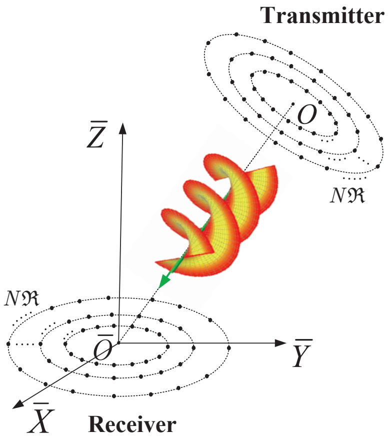

Fig. 2: The UCCA-based LoS OAM-MIMO communication system in the non-parallel misalignment case, in which the coordinate of O is (r, φ, α).

For a practical OAM communication system, a beam steering method [12] is usually applied to avoid large performance degradation caused by the misalignment between the transmitter and receiver, which requires the angle of arrival (AoA) of the OAM beam to be known. The AoA estimation and signal reception of a misaligned UCA-based OAM communication system have been studied in [13] and [14], respectively. In this paper, we consider a misaligned UCCA-based LoS multi-carrier multi-mode OAM and MIMO (MCMM-OAM-MIMO) system. Based on the utilized channel estimation and signal detection schemes, we analyze the SE and EE performances of the MCMM-OAM-MIMO system. Numerical simulation compares the EE and SE performances of the RF analog and baseband digital synthesis structures, and shows the superiority of the UCCA-based MCMM-OAM-MIMO system to the traditional MIMO-OFDM system.

II. System Model

A. Channel Model

In free space communications, the transfer function h depends on the frequency and the distance d between the transmit and receive antenna and can be expressed as [12], [15]

$$h(k,d) = \frac{\beta}{2kd}\exp\left(-ikd\right), \tag{1}$$

where $k = 2\pi/\lambda$ is the wave number, λ is the wavelength, $\frac{1}{2kd}$ denotes the degradation of amplitude, the complex exponential term is the phase difference due to the propagation distance, and β contains all relevant constants.

We assume that both the transmit and receive UCCAs consist of $\mathfrak{N}$ concentric N-element UCAs with radii $R_{t_\mathfrak{n}}$ and $R_{r_\mathfrak{m}}$, $\mathfrak{m}, \mathfrak{n} = 1, 2, \cdots, \mathfrak{N}$. In practice, it is difficult to perfectly align the transmitter and receiver. Therefore, we consider a more practical non-parallel misalignment case [14]. The coordinate of the transmit UCCA center is $\mathrm{O}(r, \varphi, \alpha)$ in $\bar{\mathrm{Z}} - \bar{\mathrm{X}}\bar{\mathrm{O}}\bar{\mathrm{Y}}$, as shown in Fig. 2, where r is the distance between the transmit and receive UCA centers, φ is the azimuth angle, α is the elevation angle, and φ and α are defined as the AoA of the received OAM beams. Then, the channel coefficients from the nth element in the $\mathfrak{n}$th transmit UCA to the mth element in the $\mathfrak{m}$th receive UCA can be expressed as $h_{\mathfrak{m},\mathfrak{n}}^{m,n} = h(k, d_{\mathfrak{m},\mathfrak{n}}^{m,n})$, where the transmission distance $d_{\mathfrak{m},\mathfrak{n}}^{m,n}$ is calculated as [14]

$$\begin{aligned} d_{\mathfrak{m},\mathfrak{n}}^{m,n} = \big[& R_{t_\mathfrak{n}}^2 + R_{r_\mathfrak{m}}^2 + r^2 + 2rR_{r_\mathfrak{m}}\cos\theta_\mathfrak{m}^m\cos\varphi\sin\alpha \\ & - 2R_{t_\mathfrak{n}}R_{r_\mathfrak{m}}(\sin\phi_\mathfrak{n}^n\sin\theta_\mathfrak{m}^m\cos\varphi + \cos\phi_\mathfrak{n}^n\cos\theta_\mathfrak{m}^m\cos\gamma) \\ & - 2R_{t_\mathfrak{n}}R_{r_\mathfrak{m}}(\sin\phi_\mathfrak{n}^n\cos\theta_\mathfrak{m}^m\sin\varphi - \cos\phi_\mathfrak{n}^n\sin\theta_\mathfrak{m}^m\sin\varphi\cos\alpha) \\ & - 2rR_{r_\mathfrak{m}}\sin\theta_\mathfrak{m}^m\sin\varphi\sin\alpha\big]^{1/2}, \end{aligned} \tag{2}$$

$\gamma = \arccos(\cos\alpha\cos\varphi)$, $\phi_\mathfrak{n}^n = [2\pi(n-1)/N + \phi_\mathfrak{n}^0]$ and $\theta_\mathfrak{m}^m = [2\pi(m-1)/N + \theta_\mathfrak{m}^0]$ are the azimuth angles of the transmit and receive elements, respectively, $\phi_\mathfrak{n}^0$ and $\theta_\mathfrak{m}^0$ are respectively the corresponding initial angles of the first reference elements, $m, n = 1, 2, \cdots, N$, $\mathfrak{m}, \mathfrak{n} = 1, 2, \cdots, \mathfrak{N}$. For simplicity, we assume $\phi_\mathfrak{n}^0 = 0$ and $\theta_\mathfrak{m}^0 = 0$ here.

Therefore, the channel matrix of the UCCA-based free space system can be expressed as $\mathbf{H}_{\text{UCCA}} = [\mathbf{H}_{\mathfrak{m},\mathfrak{n}}]_{\mathfrak{N}\times\mathfrak{N}}$, where $\mathbf{H}_{\mathfrak{m},\mathfrak{n}} = [h_{\mathfrak{m},\mathfrak{n}}^{m,n}]_{N\times N}$ is the channel matrix from the $\mathfrak{n}$th transmit UCA to the $\mathfrak{m}$th receive UCA. Note that when $\alpha = 0$ and $\varphi = 0$, $\mathbf{H}_{\mathfrak{m},\mathfrak{n}}$ is a circulant matrix and can be decomposed as $\mathbf{H}_{\mathfrak{m},\mathfrak{n}} = \mathbf{F}_N^H\mathbf{\Lambda}_{\mathfrak{m},\mathfrak{n}}\mathbf{F}_N$, where $\mathbf{F}_N$ is the N-dimensional Fourier matrix, and $\mathbf{\Lambda}_{\mathfrak{m},\mathfrak{n}}$ is a diagonal matrix whose diagonal elements are the eigenvalues of $\mathbf{H}_{\mathfrak{m},\mathfrak{n}}$.

B. Signal Model

When the CSI is unknown, it is necessary to perform a channel estimation procedure. In the UCCA-based LoS MCMM-OAM-MIMO communication system, we assume V subcarriers and U $(1 \le U \le N)$ OAM modes for data transmission as shown in Fig. 1, and $\widetilde{V}$ subcarriers and $\widetilde{U}$ OAM modes for training. Usually, $\widetilde{V} \le V$ and $\widetilde{U} \le U$.

To reduce training overhead, we only use one pair of the transmit and receive UCAs for channel estimation. Then, the equivalent baseband signal model of transmitted multiple single-mode OAM training symbols can be expressed as $\mathbf{F}_{\widetilde{U}}^H\mathbf{S}'(k_v)$, where $\mathbf{F}_{\widetilde{U}} = [\mathbf{f}^H(\ell_1),\ \mathbf{f}^H(\ell_2),\ \cdots,\ \mathbf{f}^H(\ell_{\widetilde{U}})]^H$ is a $\widetilde{U} \times N$ (partial) discrete Fourier transform (DFT) matrix, $\mathbf{f}(\ell_u) = \frac{1}{\sqrt{N}}[1,\ e^{-i\frac{2\pi\ell_u}{N}},\ \cdots,\ e^{-i\frac{2\pi\ell_u(N-1)}{N}}]$, $\mathbf{S}'(k_v) = \mathrm{diag}\{s'(\ell_1,k_v),\ s'(\ell_2,k_v),\cdots,s'(\ell_{\widetilde{U}},k_v)\}$ consists of the training symbols transmitted on $\widetilde{U}$ OAM modes at the vth $(1 \le v \le \widetilde{V})$ subcarrier sequentially. Thus, the received baseband training symbol matrix $\mathbf{Y}'(k_v)$ can be written as

$$\mathbf{Y}'(k_v) = \mathbf{H}_{\text{UCA}}(k_v)\mathbf{F}_{\widetilde{U}}^H\mathbf{S}'(k_v) + \mathbf{Z}'(k_v), \tag{3}$$

where $\mathbf{Y}'(k_v)$ is a $N \times \widetilde{U}$ matrix, $\mathbf{H}_{\text{UCA}}(k_v)$ is the channel matrix between a pair of the transmit and receive UCAs at the vth subcarrier and is selected as $\mathbf{H}_{\text{UCA}}(k_v) = [h_{1,1}^{m,n}]_{N\times N}$, and $\mathbf{Z}'(k_v)$ is the related additive Gaussian noise matrix.

Corresponding, the equivalent baseband signal model of transmitted multi-mode OAM data symbols in the UCCA-based LoS MCMM-OAM-MIMO system can be expressed as $\mathbf{I}_\mathfrak{N} \otimes \mathbf{F}_U^H\bar{\mathbf{s}}(k_v)$, where $\bar{\mathbf{s}}(k_v) = [\mathbf{s}_1^T(k_v),\ \mathbf{s}_2^T(k_v),\ \cdots,\ \mathbf{s}_\mathfrak{N}^T(k_v)]^T$, $\mathbf{s}_\mathfrak{n}(k_v) = [s_\mathfrak{n}(\ell_1,k_v),\ s_\mathfrak{n}(\ell_2,k_v),\ \cdots,\ s_\mathfrak{n}(\ell_U,k_v)]^T$ is the data symbol vector on the $\mathfrak{n}$th transmit UCA and consists of the independent data symbols transmitted on U OAM modes at the vth $(1 \le v \le V)$ subcarrier simultaneously.

Then, the received baseband data symbol vector $\bar{\mathbf{y}}(k_v)$ can be written as

$$\bar{\mathbf{y}}(k_v) = \mathbf{H}_{\text{UCCA}}(k_v)\mathbf{I}_{\mathfrak{N}} \otimes \mathbf{F}_U^H \bar{\mathbf{s}}(k_v) + \bar{\mathbf{z}}(k_v), \tag{4}$$

where $\bar{\mathbf{y}}(k_v) = [\mathbf{y}_1^T(k_v),\ \mathbf{y}_2^T(k_v),\ \cdots,\ \mathbf{y}_{\mathfrak{N}}^T(k_v)]^T$, $\mathbf{y}_{\mathfrak{m}}(k_v) = [y_{\mathfrak{m}}(1,k_v),\ y_{\mathfrak{m}}(2,k_v),\ \cdots,\ y_{\mathfrak{m}}(N,k_v)]^T$ is the received data symbol vector on the $\mathfrak{m}$th receive UCA, $\mathbf{H}_{\text{UCCA}}(k_v)$ is the channel matrix of the UCCA-based system at the vth subcarrier, and $\bar{\mathbf{z}}(k_v) = [\mathbf{z}_1^T(k_v),\ \mathbf{z}_2^T(k_v),\ \cdots,\ \mathbf{z}_{\mathfrak{N}}^T(k_v)]^T$ is the additive complex Gaussian noise vector with zero mean and covariance matrix $\sigma_{\bar{z}}^2 \mathbf{I}_{\mathfrak{N}N}$ on the receive UCCA, $\mathbf{z}_{\mathfrak{m}}(k_v) = [z_{\mathfrak{m}}(1,k_v),\ z_{\mathfrak{m}}(2,k_v),\ \cdots,\ z_{\mathfrak{m}}(N,k_v)]^T$.

At the receiver, the CSI is extracted from the received training symbol matrix $\mathbf{Y}'(k_v)$ and used for signal processing. Then, the detected data symbol vector $\bar{\mathbf{x}}(k_v)$ is expressed as

$$\bar{\mathbf{x}}(k_v) = \bar{\mathbf{D}}(k_v)\left(\mathbf{H}_{\text{UCCA}}(k_v)\mathbf{I}_{\mathfrak{N}} \otimes \mathbf{F}_U^H \bar{\mathbf{s}}(k_v) + \bar{\mathbf{z}}(k_v)\right), \tag{5}$$

where $\bar{\mathbf{x}}(k_v) = [\mathbf{x}_1^T(k_v),\ \mathbf{x}_2^T(k_v),\ \cdots,\ \mathbf{x}_{\mathfrak{N}}^T(k_v)]^T$, $\mathbf{x}_{\mathfrak{m}}(k_v) = [x_{\mathfrak{m}}(\ell_1,k_v),\ x_{\mathfrak{m}}(\ell_2,k_v),\ \cdots,\ x_{\mathfrak{m}}(\ell_U,k_v)]^T$ is the detected data symbol vector on the $\mathfrak{m}$th receive UCA, and $\bar{\mathbf{D}}(k_v)$ is a $\mathfrak{N}U \times \mathfrak{N}N$ data signal detection matrix for eliminating the effects caused by misalignment and data recovery.

C. Power Consumption Model

Based on the common power consumption model in MIMO systems [5], [6], we formulate the consumed total power as

$$P_{\text{total}} = \frac{P_{\text{T}}}{\rho} + P_{\text{c}}, \tag{6}$$

where P_{T} is the total transmit power, ρ is the efficiency of the power amplifier (PA), and P_{c} is the total circuit power consumption which is modeled as a linear function of the number of transmission antennas and the number of RF chains.

The circuit power consumptions of both the transmitter and receiver need to be considered. For the UCCA-based MCMM-OAM-MIMO system, the two receiver structures are similar to the transmitter structures shown in Fig. 1, with only the PAs being replaced by low noise amplifiers (LNAs) and the digital-to-analog converters (DACs) being replaced by analog-to-digital converters (ADCs). Therefore, for the RF analog synthesis structure, the total circuit power consists of the powers of the baseband, the RF chains, the LNAs, the phase shifters and the combiners and splitters. Since the passive combiners and splitters without power cost are considered, the total circuit power consumption of the analog synthesis structure, denoted as P_{c}^{AS}, can be expressed as

$$P_{\text{c}}^{\text{AS}} = 2P_{\text{BB}} + 2\mathfrak{N}UP_{\text{RF}} + \mathfrak{N}NP_{\text{LNA}} + 2\mathfrak{N}UNP_{\text{PS}}, \tag{7}$$

where P_{BB}, P_{RF}, P_{LNA} and P_{PS} are the powers consumed by a baseband processor, an RF chain of the transmitter/receiver, a LNA and a phase shifter, respectively, P_{RF} consists of the powers consumed by a mixer, a local oscillator, a filter and a DAC/ADC [6]. For the baseband digital synthesis structure, the total circuit power consumption includes the powers of the baseband, the RF chains and the LNAs, which is denoted as P_{c}^{DS} and takes the form

$$P_{\text{c}}^{\text{DS}} = 2P_{\text{BB}} + 2\mathfrak{N}NP_{\text{RF}} + \mathfrak{N}NP_{\text{LNA}}. \tag{8}$$

III. Channel Estimation and Signal Detection

A. Channel Estimation

According to the channel model, when N, $\mathfrak{N}$, $R_{t_{\mathfrak{n}}}$, $R_{r_{\mathfrak{m}}}$ are known, $d_{\mathfrak{m},\mathfrak{n}}^{m,n}$ in (2) is parameterized by only three parameters, that is, the distance r and the AoA α and φ. Therefore, the physical channel of the UCCA-based LoS MCMM-OAM-MIMO communication system at the vth subcarrier $\mathbf{H}_{\text{UCCA}}(k_v)$ is completely characterized by r, α and φ.

To obtain the channel parameters r, α and φ, we combine the received signals on all the N elements as follow

$$\mathbf{x}'(k_v) = \mathbf{1}^T\mathbf{Y}'(k_v) = \mathbf{1}^T\left(\mathbf{H}_{\text{UCA}}(k_v)\mathbf{F}_{\widetilde{U}}^H\mathbf{S}'(k_v) + \mathbf{Z}'(k_v)\right), \tag{9}$$

where $\mathbf{1}$ is the N-dimensional vector of ones, $\mathbf{x}'(k_v) = [x'(\ell_1,k_v),\ x'(\ell_2,k_v),\ \cdots,\ x'(\ell_{\widetilde{U}},k_v)]$. $x'(\ell_u,k_v)$ in the $\bar{\text{Z}}-\bar{\text{X}}\bar{\text{O}}\bar{\text{Y}}$ coordinate system can be derived as

$$\begin{aligned}
x'(\ell_u,k_v) &= \sum_{m=1}^{N} \mathbf{h}_{\text{UCA}}^m(k_v)\mathbf{f}^H(\ell_u)s'(\ell_u,k_v) + z'(\ell_u,k_v)\\
&= \frac{\beta}{2k_v\sqrt{N}}\sum_{m=1}^{N}\sum_{n=1}^{N}\frac{e^{ik_p|\boldsymbol{r}-\boldsymbol{r}_n'+\boldsymbol{r}_m'|}}{|\boldsymbol{r}-\boldsymbol{r}_n'+\boldsymbol{r}_m'|}e^{i\ell_u\varphi_n}s'(\ell_u,k_v)\\
&\quad + z'(\ell_u,k_v)\\
&\approx \sigma_{\ell_u,k_v} i^{-\ell_u} J_{\ell_u}(k_vR_t\sin\alpha)J_0(k_vR_r\sin\alpha)\\
&\quad e^{ik_vr}e^{i\ell_u\gamma} + z'(\ell_u,k_v),
\end{aligned} \tag{10}$$

where $u = 1,2,\cdots,\widetilde{U}$, $v = 1,2,\cdots,\widetilde{V}$, $\mathbf{h}_{\text{UCA}}^m(k_v) = [h(k_v,d_{1,1}^{m,1}),\ h(k_v,d_{1,1}^{m,2}),\ \cdots,\ h(k_v,d_{1,1}^{m,N})]$, $\boldsymbol{r}$, $\boldsymbol{r}_n'$ and $\boldsymbol{r}_m'$ are the vectors from point O to point $\bar{\text{O}}$, from point O to the nth transmit element and from point $\bar{\text{O}}$ to the mth receive element, respectively, $J_l(\cdot)$ is lth-order Bessel function of the first kind, $\sigma_{\ell_u,k_v} = \frac{\beta N^{3/2}}{2k_vr}\ s'(\ell_u,k_v)$. In (10), the approximations $|\boldsymbol{r}-\boldsymbol{r}_n'+\boldsymbol{r}_m'| \approx r$ for amplitudes and $|\boldsymbol{r}-\boldsymbol{r}_n'+\boldsymbol{r}_m'| \approx r - \hat{\boldsymbol{r}}\cdot\boldsymbol{r}_n' + \hat{\boldsymbol{r}}\cdot\boldsymbol{r}_m'$ for phases are used, where $\hat{\boldsymbol{r}}$ is the unit vector of $\boldsymbol{r}$.

Then, all the signals received on the $\widetilde{U}$ OAM modes at the $\widetilde{V}$ subcarriers are collected in the matrix $\mathbf{X}'_{\widetilde{U},\widetilde{V}} = [x'(\ell_u,k_v)]_{\widetilde{U}\times\widetilde{V}}$. When the conditions $k_{v+1}-k_v = 1$ and $\ell_{u+1}-\ell_u = 1$ are satisfied, the distance and AoA estimation method based on a single UCA [13] can be directly utilized to obtain the estimated values $\hat{r}$, $\hat{\alpha}$ and $\hat{\varphi}$. It is worth noting that using the distance and AoA estimation method the required number of training symbols of the UCCA-based LoS MCMM-OAM-MIMO system does not increase with the number of subcarriers, transmit and receive antenna elements, which is opposite in traditional MIMO-OFDM channel estimation.

B. Signal Detection

In the non-parallel misalignment case, the angles α and φ result in OAM inter-mode interferences, and thus a beam steering method [12] is applied in the UCCA-based LoS MCMM-OAM-MIMO system, which steers the beam patterns towards the direction of the incident OAM beam and thus compensates the changed phases caused by α and φ at the receive UCCA.

The receive beam steering matrix $\bar{\mathbf{B}}(k_v)$ of the UCCA-based system is represented as a block diagonal matrix whose diagonal elements are $\mathbf{B}_{\mathfrak{m}}(k_v)$, $\mathfrak{m}=1,2,\cdots,\mathfrak{N}$. $\mathbf{B}_{\mathfrak{m}}(k_v)$ represents the beam steering matrix of the $\mathfrak{m}$th receive UCA and is designed as $\mathbf{B}_{\mathfrak{m}}(k_v)=\mathbf{1}\otimes\mathbf{b}_{\mathfrak{m}}(k_v)$, where $\mathbf{1}$ is U-dimensional vector of ones, $\mathbf{b}_{\mathfrak{m}}(k_v)=[e^{iW^1_{\mathfrak{m}}(k_v)}, e^{iW^2_{\mathfrak{m}}(k_v)}, \cdots, e^{iW^N_{\mathfrak{m}}(k_v)}]$, $W^m_{\mathfrak{m}}(k_v)=k_v R_{r_{\mathfrak{m}}}(\cos\theta^m_{\mathfrak{m}}\cos\hat{\varphi}\sin\hat{\alpha}-\sin\theta^m_{\mathfrak{m}}\sin\hat{\varphi}\sin\hat{\alpha})$. After involving these phases into $\mathbf{F}_U$ at the corresponding receive UCA, the effective channel of the UCCA-based LoS MCMM-OAM-MIMO system at the vth subcarrier can be written as

$$\begin{aligned}\bar{\mathbf{H}}'_{\text{OAM-MIMO}}(k_v)&=(\mathbf{I}_{\mathfrak{N}}\otimes\mathbf{F}_U)\odot\bar{\mathbf{B}}(k_v)\mathbf{H}_{\text{UCCA}}(k_v)\mathbf{I}_{\mathfrak{N}}\otimes\mathbf{F}_U^H\\&=\left[\mathbf{H}'_{\text{OAM}_{\mathfrak{m},\mathfrak{n}}}(k_v)\right]_{\mathfrak{N}\times\mathfrak{N}},\end{aligned}\qquad(11)$$

where $\mathbf{H}'_{\text{OAM}_{\mathfrak{m},\mathfrak{n}}}(k_v)=(\mathbf{F}_U\odot\mathbf{B}_{\mathfrak{m}}(k_v))\mathbf{H}_{\mathfrak{m},\mathfrak{n}}(k_v)\mathbf{F}_U^H$ denotes the $U\times U$ effective multi-mode OAM channel from the $\mathfrak{n}$th transmit UCA to the $\mathfrak{m}$th receive UCA and is diagonal, $v=1,2,\cdots,V$. When $\hat{\alpha}$ and $\hat{\varphi}$ are sufficiently accurate, according to Theorem 1 and Theorem 2 in [14], after beam steering the inter-mode interferences induced by α and φ can be almost completely eliminated, and the diagonal elements of $\mathbf{H}'_{\text{OAM}_{\mathfrak{m},\mathfrak{n}}}(k_v)$ can be approximately obtained as

$$\begin{aligned}&h'_{\text{OAM}_{\mathfrak{m},\mathfrak{n}},k_v}(u,u)\approx\eta(k_v)\frac{N}{2^{\tau_u}}\frac{i^{\tau_u}}{\tau_u!}S^{\tau_u}_{\mathfrak{m},\mathfrak{n}}(k_v),\\&u=1,2,\cdots,U,\end{aligned}\qquad(12)$$

where $\eta(k_v)=\frac{\beta}{2k_v r}\exp(-ik_v r)$, $S^{\tau_u}_{\mathfrak{m},\mathfrak{n}}(k_v)=k_v R_{t_{\mathfrak{n}}}R_{r_{\mathfrak{m}}}/r$, and $\tau_u=\min\{|\ell_u|, N-|\ell_u|\}$.

Thus, the signal detection matrix $\bar{\mathbf{D}}(k_v)$ could be designed as the cascade of the beam steering matrix $\bar{\mathbf{B}}(k_v)$ with the estimated AoA $\hat{\alpha}$ and $\hat{\varphi}$, the despiralization matrix $\mathbf{I}_{\mathfrak{N}}\otimes\mathbf{F}_U$ and the amplitude detection matrix $\bar{\mathbf{\Gamma}}^{-1}(k_v)$ with the estimated distance $\hat{r}$ as follow

$$\bar{\mathbf{D}}(k_v)=\bar{\mathbf{\Gamma}}^{-1}(k_v)\left(\mathbf{I}_{\mathfrak{N}}\otimes\mathbf{F}_U\right)\odot\bar{\mathbf{B}}(k_v),\qquad(13)$$

where $\bar{\mathbf{\Gamma}}(k_v)=[\mathbf{\Gamma}_{\mathfrak{m},\mathfrak{n}}(k_v)]_{\mathfrak{N}\times\mathfrak{N}}$ is the matrix designed for eliminating the co-mode interferences between UCAs, $\mathbf{\Gamma}_{\mathfrak{m},\mathfrak{n}}(k_v)$ is a diagonal matrix where diagonal elements have the same form as (12) but replacing all r with $\hat{r}$. Therefore, the detected data symbol vector $\bar{\mathbf{x}}(k_v)\approx\bar{\mathbf{s}}(k_v)+\boldsymbol{\mathcal{I}}(k_v)+\hat{\bar{\mathbf{z}}}(k_v)$, where $\boldsymbol{\mathcal{I}}(k_v)=\left(\bar{\mathbf{\Gamma}}^{-1}(k_v)\bar{\mathbf{H}}'_{\text{OAM-MIMO}}(k_v)-\mathbf{I}_{\mathfrak{N}U}\right)\bar{\mathbf{s}}(k_v)$ is the remaining interferences induced by the error in detection matrix, and $\hat{\bar{\mathbf{z}}}(k_v)=\bar{\mathbf{D}}(k_v)\bar{\mathbf{z}}(k_v)$.

IV. Spectral and Energy Efficiency

Assume that T_c is the coherence time and T_v is the time spent in transmitting training symbols. According to the channel estimation and signal reception discussed above, the maximum achievable SE of the UCCA-based LoS MCMM-OAM-MIMO system can be expressed as

$$\begin{aligned}&\eta_{\text{SE}}=\left(1-\frac{T_v\tilde{V}}{T_cV\mathfrak{N}}\right)\frac{1}{V}\times\\&\sum_{v=1}^{V}\log_2\left|\mathbf{I}_{\mathfrak{N}U}+\left(\mathbf{R}^{\boldsymbol{\mathcal{I}}}(k_v)+\mathbf{R}^{\hat{\bar{\mathbf{z}}}}(k_v)\right)^{-1}\mathbf{R}^{\bar{\mathbf{s}}}(k_v)\right|,\end{aligned}\qquad(14)$$

where $\mathbf{R}^{\bar{\mathbf{s}}}(k_v)$, $\mathbf{R}^{\boldsymbol{\mathcal{I}}}(k_v)$ and $\mathbf{R}^{\hat{\bar{\mathbf{z}}}}(k_v)$ are the $\mathfrak{N}U\times\mathfrak{N}U$ correlation matrices of the signal vector, the interference vector and the noise vector, respectively. We consider equal power allocation and denote the transmit power at each subcarrier and each transmit UCA as P_{t}. Then, $\mathbf{R}^{\bar{\mathbf{s}}}(k_v)$, $\mathbf{R}^{\boldsymbol{\mathcal{I}}}(k_v)$ and $\mathbf{R}^{\hat{\bar{\mathbf{z}}}}(k_v)$ can be calculated as

$$\mathbf{R}^{\bar{\mathbf{s}}}(k_v)=\mathbb{E}\left[\bar{\mathbf{s}}(k_v)\bar{\mathbf{s}}^H(k_v)\right]=\frac{P_{\text{t}}}{U}\mathbf{I}_{\mathfrak{N}U},\qquad(15)$$

$$\begin{aligned}\mathbf{R}^{\boldsymbol{\mathcal{I}}}(k_v)&=\left(\bar{\mathbf{\Gamma}}^{-1}(k_v)\bar{\mathbf{H}}'_{\text{OAM-MIMO}}(k_v)-\mathbf{I}_{\mathfrak{N}U}\right)\mathbb{E}\left[\bar{\mathbf{s}}(k_v)\bar{\mathbf{s}}^H(k_v)\right]\\&\quad\left(\bar{\mathbf{\Gamma}}^{-1}(k_v)\bar{\mathbf{H}}'_{\text{OAM-MIMO}}(k_v)-\mathbf{I}_{\mathfrak{N}U}\right)^H,\\&=\frac{P_{\text{t}}}{U}\left(\bar{\mathbf{\Gamma}}^{-1}(k_v)\bar{\mathbf{H}}'_{\text{OAM-MIMO}}(k_v)-\mathbf{I}_{\mathfrak{N}U}\right)\\&\quad\left(\bar{\mathbf{\Gamma}}^{-1}(k_v)\bar{\mathbf{H}}'_{\text{OAM-MIMO}}(k_v)-\mathbf{I}_{\mathfrak{N}U}\right)^H,\end{aligned}\qquad(16)$$

and

$$\begin{aligned}\mathbf{R}^{\hat{\bar{\mathbf{z}}}}(k_v)&=\bar{\mathbf{D}}(k_v)\mathbb{E}\left[\bar{\mathbf{z}}(k_v)\bar{\mathbf{z}}^H(k_v)\right]\bar{\mathbf{D}}^H(k_v)\\&=\sigma^2_{\bar{z}}\bar{\mathbf{D}}(k_v)\bar{\mathbf{D}}^H(k_v).\end{aligned}\qquad(17)$$

Using (13), (17) can be further simplified as

$$\begin{aligned}\mathbf{R}^{\hat{\bar{\mathbf{z}}}}(k_v)&=\sigma^2_{\bar{z}}\bar{\mathbf{\Gamma}}^{-1}(k_v)\left((\mathbf{I}_{\mathfrak{N}}\otimes\mathbf{F}_U)\odot\bar{\mathbf{B}}(k_v)\right)\\&\quad\left((\mathbf{I}_{\mathfrak{N}}\otimes\mathbf{F}_U)\odot\bar{\mathbf{B}}(k_p)\right)^H\left(\bar{\mathbf{\Gamma}}^{-1}(k_p)\right)^H\\&=\sigma^2_{\bar{z}}\left(\bar{\mathbf{\Gamma}}^H(k_v)\bar{\mathbf{\Gamma}}(k_v)\right)^{-1}.\end{aligned}\qquad(18)$$

When the received SNR is enough high, the estimates $\hat{r}$, $\hat{\alpha}$ and $\hat{\varphi}$ are sufficiently accurate. Then, according to the design of the matrix $\bar{\mathbf{\Gamma}}^{-1}(k_v)$, the following approximations holds

$$\bar{\mathbf{\Gamma}}^{-1}(k_v)\bar{\mathbf{H}}'_{\text{OAM-MIMO}}(k_v)\approx\mathbf{I}_{\mathfrak{N}U},\ \ \mathbf{R}^{\boldsymbol{\mathcal{I}}}(k_v)\approx\mathbf{0}.\qquad(19)$$

Under this condition, the maximum achievable SE in (14) can be reformulated as

$$\eta_{\text{SE}}\approx\left(1-\frac{T_v\tilde{V}}{T_cV\mathfrak{N}}\right)\frac{1}{V}\sum_{v=1}^{V}\log_2\left|\mathbf{I}_{\mathfrak{N}U}+\frac{P_{\text{t}}}{\sigma^2_{\bar{z}}U}\bar{\mathbf{\Gamma}}^H(k_v)\bar{\mathbf{\Gamma}}(k_v)\right|.\qquad(20)$$

According to the definition as the ratio of the capacity to the total system power consumption, the EE of the UCCA-based LoS MCMM-OAM-MIMO system can be written as

$$\eta_{\text{EE}}=\frac{B\eta_{\text{SE}}}{P_{\text{total}}}=\frac{B\eta_{\text{SE}}}{P_{\text{T}}/\rho+P_{\text{c}}},\qquad(21)$$

where B is the system available bandwidth, the total transmit power $P_{\text{T}}=\mathfrak{N}VP_{\text{t}}$, and the total circuit power consumption P_{c} of the RF analog synthesis and baseband digital synthesis structures are shown in (7) and (8), respectively.

V. Numerical Results

In this section, the EE and SE performances of the UCCA-based LoS MCMM-OAM-MIMO communication system are illustrated and compared with that of the traditional LoS MIMO-OFDM system. We consider a UCCA-based system in the non-parallel misalignment with the elevation angle $\alpha=7^\circ$ and the azimuth angle $\varphi=7^\circ$. Both the transmitter and receiver consists of $\mathfrak{N}=4$ concentric UCAs each having $N=16$ antenna elements, and the distance between the transmit and receive UCCA centers is set as $r=4$m. The constant β is set to 16dB.

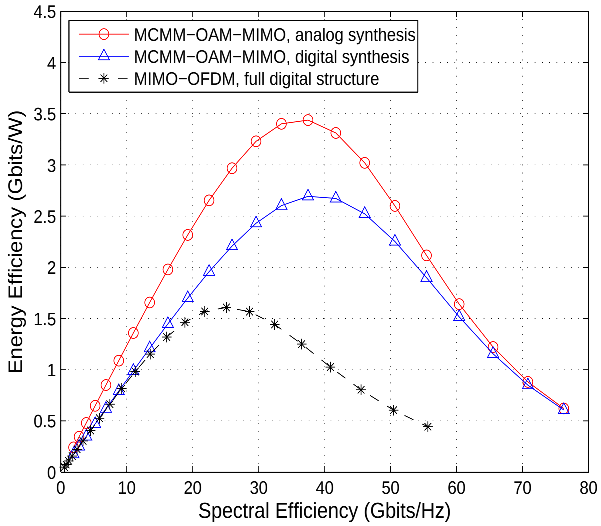

Fig. 3: The EE-SE relationships of the UCCA-based LoS MCMM-OAM-MIMO system implemented by RF analog synthesis and baseband digital synthesis and the traditional LoS MIMO-OFDM system with full digital structure.

In the simulation, T_c is assumed to be 256 OFDM symbols, the number of subcarriers and OAM modes for data transmission are assumed to be $V = 64$ and $U = 5$ ($\ell = 0, \pm 1, \pm 2$), respectively. To meet the conditions of the distance and AoA estimation method, that is, $k_{v+1} - k_v = 1$ and $\ell_{u+1} - \ell_u = 1$ ($1 \leq v \leq \widetilde{V}, 1 \leq u \leq \widetilde{U}$), the subcarrier interval should be $\triangle f_k = 47.7$MHz. We choose $\widetilde{V} = 8$ subcarriers from 2.244GHz to 2.578GHz corresponding to the wave numbers $k_1, k_2, \cdots, k_8 = 47, 48, \ldots, 54$, and $\widetilde{U} = 4$ OAM modes with $\ell_1, \ell_2, \ell_3, \ell_4 = -2, -1, 0, +1$ for training. And $R_t = R_r = 1.5\lambda_1,\ 2\lambda_1,\ 2.5\lambda_1,\ 3\lambda_1,\ \lambda_1 = 2\pi/k_1$. Thus, the channel estimation of the MCMM-OAM-MIMO system only requires $\widetilde{U} = 4$ training symbols per subcarrier, while the traditional MIMO-OFDM system channel estimation requires $\mathfrak{N}N = 64$ training symbols per subcarrier. Referring to the selection of parameters in [6] and [16], the overall power consumption of an RF chain is approximately assumed to be 250mW, and the power consumed by other circuit components are set as $P_{\text{BB}} = 200$mW, $P_{\text{LNA}} = 20$mW and $P_{\text{PS}} = 20$mW.

Fig. 3 shows the EE-SE relationships of the UCCA-based LoS MCMM-OAM-MIMO system and the LoS MIMO-OFDM system. It is obvious that the MCMM-OAM-MIMO system implemented by analog synthesis is more energy-efficient than the system implemented by digital synthesis because of fewer RF chains when part of the available OAM modes are used. In addition, we can observe from the figure that there are tradeoffs between EEs and SEs, but compared with the MIMO-OFDM system, the MCMM-OAM-MIMO system can achieve much higher EE in a large range of SE.

VI. Conclusions

In this correspondence, we investigate the SE and EE of a misaligned UCCA-based LoS MCMM-OAM-MIMO system, where a distance and AoA estimation method based on a single UCA is used for channel estimation, and a signal detection scheme including beam steering with the estimated AoA for eliminating the interferencs caused by misalignment and amplitude detection with the estimated distance for data recovery is utilized. Two transceiver structures, RF analog synthesis structure and baseband digital synthesis structure under a common linear power consumption model are considered, based on which the EE and SE performances of the UCCA-based LoS MCMM-OAM-MIMO system are investigated. The RF analog synthesis structure of MCMM-OAM-MIMO system is more energy-efficient than its baseband digital synthesis structure, which are both superior to the traditional LoS MIMO-OFDM system in the EE and SE performances.

References

[1] L. Allen, M. W. Beijersbergen, R. J. Spreeuw, and J. P. Woerdman, "Orbital angular momentum of light and the transformation of Laguerre-Gaussian laser modes," *Phys. Rev. A: At. Mol. Opt. Phys.*, vol. 45, no. 11, pp. 8185–8189, 1992.

[2] S. M. Mohammadi, L. K. S. Daldorff, J. E. S. Bergman, R. L. Karlsson, B. Thidé, K. Forozesh, T. D. Carozzi, and B. Isham, "Orbital angular momentum in radio–a system study," *IEEE Trans. Antennas Propag.*, vol. 58, no. 2, pp. 565–572, Feb. 2010.

[3] Y. Yan, G. Xie, M. P. J. Lavery, H. Huang, N. Ahmed, C. Bao, Y. Ren, Y. Cao, L. Li, Z. Zhao, A. F. Molisch, M. Tur, M. J. Padgett, and A. E. Willner, "High-capacity millimetre-wave communications with orbital angular momentum multiplexing," *Nature Commun.*, vol. 5, p. 4876, Sep. 2014.

[4] Y. Ren, L. Li, G. Xie, Y. Yan, Y. Cao, H. Huang, N. Ahmed, Z. Zhao, P. Liao, C. Zhang, G. Caire, A. F. Molisch, M. Tur, and A. E. Willner, "Line-of-sight millimeter-wave communications using orbital angular momentum multiplexing combined with conventional spatial multiplexing," *IEEE Trans. Wireless Commun.*, vol. 16, no. 5, pp. 3151–3161, May 2017.

[5] G. Y. Li, Z. Xu, C. Xiong, C. Yang, S. Zhang, Y. Chen, and S. Xu, "Energy-efficient wireless communications: tutorial, survey, and open issues," *IEEE Wireless Commun.*, vol. 18, no. 6, pp. 28–35, Dec. 2011.

[6] C. Lin and G. Y. Li, "Energy-efficient design of indoor mmWave and sub-THz systems with antenna arrays," *IEEE Trans. Wireless Commun.*, vol. 15, no. 7, pp. 4660–4672, Jul. 2016.

[7] X. Ge, R. Zi, X. Xiong, Q. Li, and L. Wang, "Millimeter wave communications with OAM-SM scheme for future mobile networks," *IEEE J. Sel. Areas Commun.*, vol. 35, no. 9, pp. 2163–2177, Sep. 2017.

[8] R. Chen, H. Zhou, M. Moretti, X. Wang, and J. Li, "Orbital angular momentum waves: Generation, detection and emerging applications," *IEEE Commun. Surveys Tuts.*, pp. 1–30, Nov. 2019.

[9] W. Zhang, S. Zheng, X. Hui, R. Dong, X. Jin, H. Chi, and X. Zhang, "Mode division multiplexing communication using microwave orbital angular momentum: An experimental study," *IEEE Trans. Wireless Commun.*, vol. 16, no. 2, pp. 1308–1318, Feb. 2017.

[10] R. Chen, W. Yang, H. Xu, and J. Li, "A 2-D FFT-based transceiver architecture for OAM-OFDM systems with UCA antennas," *IEEE Trans. Veh. Technol.*, vol. 67, no. 6, pp. 5481–5485, Jun. 2018.

[11] D. Lee, H. Sasaki, H. Fukumoto, Y. Yagi, T. Kaho, H. Shiba, and T. Shimizu, "An experimental demonstration of 28 GHz band wireless OAM-MIMO (orbital angular momentum multi-input and multi-output) multiplexing," in *Proc. IEEE 85th Veh. Technol. Conf.*, 2018, pp. 1–5.

[12] R. Chen, H. Xu, M. Moretti, and J. Li, "Beam steering for the misalignment in UCA-based OAM communication systems," *IEEE Wireless Commun. Lett.*, vol. 7, no. 4, pp. 582–585, Aug. 2018.

[13] R. Chen, W.-X. Long, X. Wang, and J. Li, "Multi-mode OAM radio waves: Generation, angle of arrival estimation and reception with UCAs," *submitted to IEEE Trans. Wireless Commun.*, Dec. 2019.

[14] R. Chen, W.-X. Long, and J. Li, "Reception of misaligned multi-mode OAM signals," in *Proc. IEEE Global Commun. Conf.*, 2019, pp. 1–5.

[15] O. Edfors and A. J. Johansson, "Is orbital angular momentum (OAM) based radio communication an unexploited area?" *IEEE Trans. Antennas Propag.*, vol. 60, no. 2, pp. 1126–1131, Feb. 2012.

[16] R. Méndez-Rial, C. Rusu, N. González-Prelcic, A. Alkhateeb, and R. W. Heath, “Hybrid MIMO architectures for millimeter wave communications: Phase shifters or switches?” *IEEE Access*, vol. 4, pp. 247–267, Jan. 2016.